DTU Library

Efficient Calculation of Born Scattering for Fixed-Offset Ground-Penetrating Radar Surveys

Meincke, Peter

Link back to DTU Orbit

Efficient Calculation of Born Scattering for Fixed-Offset Ground-Penetrating Radar Surveys

Peter Meincke, *Member, IEEE*

Abstract—A formulation is presented for efficient calculation of linear electromagnetic scattering by buried penetrable objects, as involved in the analysis of fixed-offset ground-penetrating radar (GPR) systems. The actual radiation patterns of the GPR antennas are incorporated in the scattering calculation by using their plane-wave transmitting and receiving spectra.

Index Terms—Born approximation, buried objects, fixed offset, ground-penetrating radar (GPR), microwave imaging, plane-wave transmitting and receiving spectra, scattering.

I. INTRODUCTION

SIGNAL-PROCESSING algorithms based on linear inverse scattering are often used for ground-penetrating radar (GPR) imaging [1]–[8]. To validate and investigate the performance of such algorithms, an efficient calculation of the linear electromagnetic scattering by buried objects—obtained by using the first Born approximation—is essential. However, most GPR systems operate in a fixed-offset mode in which the transmitter and receiver move together, so that a new scattering problem must be solved for each new receiver location. Hence, a straightforward implementation of the Born scattering formulation is too time consuming for analysis of realistic fixed-offset GPR surveys.

In this letter, we derive an efficient formulation for calculating Born scattering by buried dielectric objects in a fixed-offset GPR configuration. Since the formulation is based on plane-wave expansions, it can be efficiently calculated using fast Fourier transforms (FFTs). Also, we include the actual radiation patterns of the GPR antennas by using their plane-wave transmitting and receiving spectra [9]. The fact that the presence of the air–soil interface impacts the radiation patterns of the antennas is accounted for by the transmitting and receiving spectra.

Throughout this letter, the time factor $\exp(-i\omega t)$ is assumed and suppressed.

II. FIXED-OFFSET GPR CONFIGURATION

The GPR configuration involving the planar air–soil interface is shown in Fig. 1. A Cartesian xyz coordinate system is introduced so that the xy plane coincides with the interface, and so that $z \geq 0$ is air, and $z < 0$ is soil. The air has permittivity ϵ_0, permeability μ_0, and wavenumber $k_0 = \omega\sqrt{\mu_0\epsilon_0}$. The
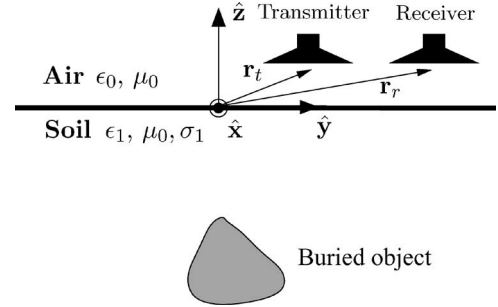
Fig. 1. Fixed-offset GPR configuration in which $\mathbf{r}_t = \mathbf{r}_r + \mathbf{r}_\Delta$ with $\mathbf{r}_\Delta$ is fixed.

soil has permittivity ϵ_1, conductivity σ_1, permeability μ_0, and wavenumber $k_1 = \sqrt{\omega^2\mu_0\epsilon_1 + i\omega\mu_0\sigma_1}$. The position of the receiving antenna is $\mathbf{r}_r = x_r\hat{\mathbf{x}} + y_r\hat{\mathbf{y}} + z_r\hat{\mathbf{z}}$ with $z_r \geq 0$, and the position of the transmitting antenna is $\mathbf{r}_t = \mathbf{r}_r + \mathbf{r}_\Delta$ with $\mathbf{r}_\Delta = x_\Delta\hat{\mathbf{x}} + y_\Delta\hat{\mathbf{y}}$ being fixed. Below the air–soil interface, penetrable objects of volume V_s are buried. The transmitting antenna is attached to a coaxial cable. In a given reference plane in the cable, the voltage between the inner and outer conductor of the field propagating toward the antenna in the cable is V_t. The background field $\mathbf{E}^{\mathrm{b}}$, which is defined as the field that would exist in the region $z < 0$ in the absence of the objects, is then expressed in terms of the plane-wave transmitting spectrum $\mathbf{T}$ of the GPR antenna as [9]

$$\mathbf{E}^{\mathrm{b}}(\mathbf{r}) = \frac{V_t}{(2\pi)^2} \iint\limits_{-\infty}^{\infty} \mathbf{T}(k_x, k_y) \exp\left(i\left[k_x(x - x_r - x_\Delta)\right.\right.$$
$$\left.\left. + k_y(y - y_r - y_\Delta) - \gamma_1 z\right]\right) dk_x dk_y \quad (1)$$

where $\mathbf{r} = x\hat{\mathbf{x}} + y\hat{\mathbf{y}} + z\hat{\mathbf{z}}$ with $z < 0$ being the position vector, and $\gamma_1 = \gamma_1(k_x, k_y) = \sqrt{k_1^2 - k_x^2 - k_y^2}$, with $\mathrm{Im}\gamma_1 \geq 0$ being the z component of the propagation vector in the soil. As described in [9], the plane-wave transmitting spectrum $\mathbf{T}$ of the GPR antenna can be determined either from the current density on the antenna or by measurements using a buried probe [10]. Here, we use the former approach and assume that $\mathbf{J}(\mathbf{r})$ is the electric current density on the antenna when it is located at the position $z_t\hat{\mathbf{z}}$. The plane-wave transmitting spectrum is then [9]

$$\mathbf{T}(k_x, k_y) = -\frac{\omega\mu_0}{2V_t}\bar{\mathbf{F}}(k_x, k_y) \cdot \tilde{\mathbf{J}}\left(\mathbf{k}_0^-\right) \quad (2)$$

where $\mathbf{k}_0^- = k_x\hat{\mathbf{x}} + k_y\hat{\mathbf{y}} - \gamma_0\hat{\mathbf{z}}$, $\gamma_0 = \gamma_0(k_x, k_y) = \sqrt{k_0^2 - k_x^2 - k_y^2}$, and $\mathrm{Im}\gamma_0 \geq 0$. Moreover, $\tilde{\mathbf{J}}$ is the

three-dimensional (3-D) spatial Fourier transform of the electric current density given by

$$\tilde{\mathbf{J}}(\mathbf{k}) = \int_{z \geq 0} \mathbf{J}(\mathbf{r}) \exp(-i\mathbf{k} \cdot \mathbf{r}) \, d^3\mathbf{r} \qquad (3)$$

where $\mathbf{k} = k_x\hat{\mathbf{x}} + k_y\hat{\mathbf{y}} + k_z\hat{\mathbf{z}}$. The dyadic $\bar{\mathbf{F}}$ in (2) is related to the dyadic Green's function of a two-layer medium in the spectral domain and is given by

$$\bar{\mathbf{F}}(k_x, k_y) = \frac{2}{(\gamma_0 + \gamma_1)\left(k_x^2 + k_y^2 + \gamma_0\gamma_1\right)}$$
$$\cdot \left[\hat{\mathbf{x}}\left(\left(k_y^2 + \gamma_0\gamma_1\right)\hat{\mathbf{x}} - k_x k_y\hat{\mathbf{y}} + k_x\gamma_1\hat{\mathbf{z}}\right)\right.$$
$$+ \hat{\mathbf{y}}\left(-k_x k_y\hat{\mathbf{x}} + \left(k_x^2 + \gamma_0\gamma_1\right)\hat{\mathbf{y}} + k_y\gamma_1\hat{\mathbf{z}}\right)$$
$$\left. + \hat{\mathbf{z}}\left(k_x\gamma_0\hat{\mathbf{x}} + k_y\gamma_0\hat{\mathbf{y}} + \left(k_x^2 + k_y^2\right)\hat{\mathbf{z}}\right)\right]. \quad (4)$$

If the antenna is described by a magnetic current density $\mathbf{M}(\mathbf{r})$, when it is located at the position $z_t\hat{\mathbf{z}}$, the plane-wave transmitting spectrum is given by

$$\mathbf{T}(k_x, k_y) = -\frac{1}{2V_t}\left[\mathbf{k}_1^- \times \bar{\mathbf{F}}(k_x, k_y)\right] \cdot \tilde{\mathbf{M}}(\mathbf{k}_0^-) \qquad (5)$$

where $\mathbf{k}_1^- = k_x\hat{\mathbf{x}} + k_y\hat{\mathbf{y}} - \gamma_1\hat{\mathbf{z}}$.

III. BORN SCATTERING BY BURIED OBJECTS

The receiving antenna of the GPR is connected to a matched receiver through a coaxial cable with characteristic admittance Y_0. In a given reference plane in the cable, the voltage V between the inner and outer conductors of the field propagating away from the antenna in the cable is [9]

$$V(\mathbf{r}_r) = \frac{1}{(2\pi)^2} \iint_{-\infty}^{\infty} \mathbf{R}(k_x, k_y) \cdot \mathbf{S}_1^+(k_x, k_y)$$
$$\cdot \exp\left(i\left[k_x x_r + k_y y_r\right]\right) dk_x dk_y \quad (6)$$

where $\mathbf{R}(k_x, k_y)$ is the plane-wave receiving spectrum of the GPR antenna, which will be discussed below after (11), and $\mathbf{S}_1^+(k_x, k_y)$ is the plane-wave spectrum of the upward-propagating field $\mathbf{E}_1^+$ in the soil. The plane-wave spectrum $\mathbf{S}_1^+(k_x, k_y)$ is determined by first considering the field $\mathbf{E}_1^+$. Under the first Born approximation, this field is identical to the scattered field $\mathbf{E}^s$ in the soil above the buried object, which is determined by [11, p. 485]

$$\mathbf{E}^s(\mathbf{r}) = i\omega\mu_0 \int_{V_s} \bar{\mathbf{G}}(\mathbf{r}, \mathbf{r}') \cdot \mathbf{E}^b(\mathbf{r}')O(\mathbf{r}')d^3\mathbf{r}' \qquad (7)$$

where $z < 0$, $z > z'$, $\mathbf{r}' = x'\hat{\mathbf{x}} + y'\hat{\mathbf{y}} + z'\hat{\mathbf{z}}$, and $O(\mathbf{r})$ is the object function describing the contrast in the electromagnetic properties from those of the background

$$O(\mathbf{r}) = \sigma(\mathbf{r}) - \sigma_1 - i\omega\left(\epsilon(\mathbf{r}) - \epsilon_1\right). \qquad (8)$$

Herein, $\epsilon(\mathbf{r})$ and $\sigma(\mathbf{r})$ are the permittivity and conductivity distributions, respectively. Furthermore, $\bar{\mathbf{G}}(\mathbf{r}, \mathbf{r}')$ in (7) is

the dyadic Green's function for a homogeneous medium with wavenumber k_1 [11, p. 381]

$$\bar{\mathbf{G}}(\mathbf{r}, \mathbf{r}') = \left(\bar{\mathbf{I}} + \frac{\nabla\nabla}{k_1^2}\right)g(\mathbf{r}, \mathbf{r}') \quad z > z' \qquad (9)$$

where $g(\mathbf{r}, \mathbf{r}')$ is the usual scalar 3-D Green's function for a homogeneous medium

$$g(\mathbf{r}, \mathbf{r}') = \frac{\exp\left(ik_1|\mathbf{r} - \mathbf{r}'|\right)}{4\pi|\mathbf{r} - \mathbf{r}'|}. \qquad (10)$$

The dyadic Green's function in (9) does not involve contributions due to the reflection in the interface since these contributions are neglected when applying the first Born approximation. The second step to obtain $\mathbf{S}_1^+(k_x, k_y)$ is to insert the plane-wave expansion of the dyadic Green's function (9) [11, p. 384] into (7) for $\mathbf{E}^s$, yielding

$$\mathbf{S}_1^+(k_x, k_y) = \frac{-\omega\mu_0}{2\gamma_1}\left(\bar{\mathbf{I}} - \frac{\mathbf{k}_1\mathbf{k}_1}{k_1^2}\right) \cdot \widetilde{[O\mathbf{E}^b]}(\mathbf{k}_1). \qquad (11)$$

Herein, $\mathbf{k}_1 = k_x\hat{\mathbf{x}} + k_y\hat{\mathbf{y}} + \gamma_1\hat{\mathbf{z}}$, and $\widetilde{[O\mathbf{E}^b]}$ is the 3-D spatial Fourier transform of the product $O(\mathbf{r})\mathbf{E}^b(\mathbf{r})$.

The plane-wave receiving spectrum $\mathbf{R}(k_x, k_y)$ in (6) satisfies that $\mathbf{R}(k_x, k_y) \cdot \mathbf{k}_1 = 0$ [9]. For a reciprocal GPR antenna, the receiving spectrum is related to the transmitting spectrum $\mathbf{T}_r(k_x, k_y)$ of the receiving GPR antenna, defined as in (1) with V_t replaced by V_{tr}, as [9]

$$\mathbf{R}(k_x, k_y) = \frac{\gamma_1}{\omega\mu_0 Y_0}\mathbf{T}_r(-k_x, -k_y). \qquad (12)$$

The final expression for the output voltage V is obtained by inserting the plane-wave spectrum (11) into (6)

$$V(\mathbf{r}_r) = \frac{-\omega\mu_0}{8\pi^2} \iint_{-\infty}^{\infty} \frac{1}{\gamma_1}\mathbf{R}(k_x, k_y) \cdot \widetilde{[O\mathbf{E}^b]}(\mathbf{k}_1)$$
$$\cdot \exp\left(i[k_x x_r + k_y y_r]\right) dk_x \, dk_y \quad (13)$$

where the fact that $\mathbf{R}(k_x, k_y) \cdot \mathbf{k}_1 = 0$ has been applied. Note that the background field $\mathbf{E}^b$ changes when the radar is moved, and therefore, $\mathbf{E}^b$ needs to be recalculated for each new location of the receiving antenna. Hence, with N_z denoting the number of grid points used to discretize the object function along the z axis and T_0 being the average calculation time of one operation in the two-dimensional (2-D) FFT, the asymptotic calculation time for the straightforward evaluation of (13) for $N_x \times N_y$ values of x_r, y_r on an $N_x \times N_y$ rectangular grid is $6N_z T_0 N_x^2 N_y^2 \log_2(N_x N_y)$ as $N_x, N_y \to \infty$. Consequently, this calculation scheme is very inefficient for fixed-offset configurations. In the following section, an efficient method is derived to deal with the considered fixed-offset case.

IV. DERIVING THE EFFICIENT FORMULATION

To derive the efficient method, insert first the expression (1) for the background field $\mathbf{E}^b$, with k_x, k_y replaced by k_x', k_y', into the relation (13) for the output voltage. Second, inspired by

the procedure in [12], interchange the integrations over k_x, k_y and k'_x, k'_y and carry out the substitutions $k''_x = k_x - k'_x$ and $k''_y = k_y - k'_y$. The result is

$$V(\mathbf{r}_r) = \iint\limits_{-\infty}^{\infty} F(k''_x, k''_y) \exp\big(i\left[k''_x x_r + k''_y y_r\right]\big)\, dk''_x dk''_y \quad (14)$$

with

$$F\left(k''_x, k''_y\right) = \int\limits_{z' \in V_s} H\left(k''_x, k''_y, z'\right) S\left(k''_x, k''_y, z'\right) dz' \quad (15)$$

$$H\left(k''_x, k''_y, z'\right) = \iint\limits_{(x', y') \in V_s} O(\mathbf{r}')$$
$$\cdot \exp\left(-i\left[k''_x x' + k''_y y'\right]\right) dx' dy' \quad (16)$$

$$S\left(k''_x, k''_y, z'\right) = \iint\limits_{-\infty}^{\infty} \mathbf{C}_1\left(k_x, k_y, z'\right)$$
$$\cdot \mathbf{C}_2\left(k''_x - k_x, k''_y - k_y, z'\right) dk_x dk_y \quad (17)$$

$$\mathbf{C}_1\left(k_x, k_y, z'\right) = \frac{-\omega\mu_0 V_t}{32\pi^4 \gamma_1} \mathbf{R}(k_x, k_y) \exp\left(-i\gamma_1 z'\right) \quad (18)$$

and

$$\mathbf{C}_2\left(k_x, k_y, z'\right) = \exp\left(i\left[k_x x_\Delta + k_y y_\Delta - \gamma_1 z'\right]\right) \mathbf{T}(-k_x, -k_y). \quad (19)$$

The integrations over k''_x, k''_y in (14) for V can be determined for all needed receiver locations using one single 2-D FFT. The relation for H in (16) can be calculated analytically for simple object functions, or otherwise by 2-D FFTs for each z' and for all needed values of k''_x, k''_y. The integrations over k_x, k_y of the dot product $\mathbf{C}_1(k_x, k_y, z') \cdot \mathbf{C}_2(k''_x - k_x, k''_y - k_y, z')$ in (17) for S are in convolutional form, and therefore, for a fixed z', $S(k''_x, k''_y, z')$ can be calculated for all needed values of k''_x and k''_y using 2-D FFTs as follows:

$$S\left(k''_x, k''_y, z'\right) = (2\pi)^2 \iint\limits_{-\infty}^{\infty} \tilde{\mathbf{C}}_1(x, y, z')$$
$$\cdot \tilde{\mathbf{C}}_2(x, y, z') \exp\left(-i\left[k''_x x + k''_y y\right]\right) dx\, dy \quad (20)$$

where

$$\tilde{\mathbf{C}}_1(x, y, z') = \frac{1}{(2\pi)^2} \iint\limits_{-\infty}^{\infty} \mathbf{C}_1\left(k_x, k_y, z'\right)$$
$$\cdot \exp\left(i\left[k_x x + k_y y\right]\right) dk_x\, dk_y \quad (21)$$

and similarly for $\tilde{\mathbf{C}}_2$. The functions $\mathbf{C}_1$ and $\mathbf{C}_2$ in (18) and (19) contain the factor $\exp(-i\gamma_1 z')$, which is exponentially decaying for $k_x^2 + k_y^2 > \operatorname{Re} k_1^2$. Hence, $\mathbf{C}_1$ and $\mathbf{C}_2$ are spatially bandlimited with the bandwidth k_{max} determined by requiring that $\exp(-\sqrt{k_{max}^2 - k_1^2}|z'|)$, with $k_{max} > \operatorname{Re} k_1$, is sufficiently small. The integrations over k_x, k_y in (17) extend over the ranges $-k_{max} < k_x < k_{max}$ and $-k_{max} < k_y < k_{max}$. Equations (15) and (17) then show that the functions

$F(k''_x, k''_y)$ and $S(k''_x, k''_y, z')$ are bandlimited with the bandwidth $2k_{max}$. Hence, the grid, on which the output voltage (14) is calculated using FFTs, has the spacing $\Delta x_r = \Delta y_r = \pi/(2k_{max})$. Assuming the worst case scenario, in which no closed-form expression exists for H in (16) and 2-D FFTs therefore are needed for its evaluation, the asymptotic calculation time for (14) equals $(1 + 8N_z)T_0 N_x N_y \log_2(N_x N_y)$ as $N_x, N_y \to \infty$, where N_x, N_y, N_z, and T_0 are defined in the previous section. Hence, the efficient formulation is $6N_x N_y N_z/(1 + 8N_z) \approx 0.75 N_x N_y$ times faster than the straightforward approach in (13).

A. 2.5-Dimensional Case

In GPR analysis, it is often of interest to calculate scattering by buried objects that are invariant in one direction. This is, for instance, the case for pipes. In the 2.5-dimensional (2.5-D) case considered in this section, it is assumed that the buried object is invariant in the $\hat{\mathbf{x}}$ direction, and that the antennas are $\hat{\mathbf{x}}$-directed Hertzian dipoles. The $\hat{\mathbf{x}}$-polarized antennas are considered for simplicity, but without loss of generality; other antenna polarization can easily be analyzed as well. The 2.5-D versions of (14)–(19) become

$$V(y_r) = \int\limits_{-\infty}^{\infty} F(k''_y) \exp\left(ik''_y y_r\right) dk''_y \quad (22)$$

$$F(k''_y) = 2\pi \int\limits_{z' \in V_s} H\left(k''_y, z'\right) S\left(k''_y, z'\right) dz' \quad (23)$$

$$H\left(k''_y, z'\right) = \int\limits_{y' \in V_s} O(y', z') \exp\left(-ik''_y y'\right) dy' \quad (24)$$

$$S\left(k''_y, z'\right) = \iint\limits_{-\infty}^{\infty} \mathbf{C}_1\left(k_x, k_y, z'\right)$$
$$\cdot \mathbf{C}_2\left(-k_x, k''_y - k_y, z'\right) dk_x\, dk_y$$
$$= (2\pi)^2 \iint\limits_{-\infty}^{\infty} \tilde{\mathbf{C}}_1(x, y, z')$$
$$\cdot \tilde{\mathbf{C}}_2(x, y, z') \exp\left(-ik''_y y\right) dx\, dy \quad (25)$$

where $\tilde{\mathbf{C}}_1$ and $\tilde{\mathbf{C}}_2$ are defined according to (21) and hence

$$\mathbf{C}_1(k_x, k_y, z) = \omega\mu_0 V_t \exp\left(i\left[\gamma_0 z_r - \gamma_1 z'\right]\right)$$
$$\cdot \left(32\pi^4 Y_0 V_{tr}(\gamma_0 + \gamma_1)\left(k_x^2 + k_y^2 + \gamma_0\gamma_1\right)\right)^{-1}$$
$$\cdot \left(\hat{\mathbf{x}}\left(k_y^2 + \gamma_0\gamma_1\right) - \hat{\mathbf{y}}k_x k_y - \hat{\mathbf{z}}k_x\gamma_0\right) \quad (26)$$

$$\mathbf{C}_2(k_x, k_y, z') = -\omega\mu_0\left(V_t(\gamma_0 + \gamma_1)\right.$$
$$\cdot \left(k_x^2 + k_y^2 + \gamma_0\gamma_1\right))^{-1}$$
$$\cdot \exp(i\left[k_x x_\Delta + k_y y_\Delta + \gamma_0 z_r - \gamma_1 z'\right])$$
$$\cdot \left(\hat{\mathbf{x}}\left(k_y^2 + \gamma_0\gamma_1\right) - \hat{\mathbf{y}}k_x k_y - \hat{\mathbf{z}}k_x\gamma_0\right). \quad (27)$$
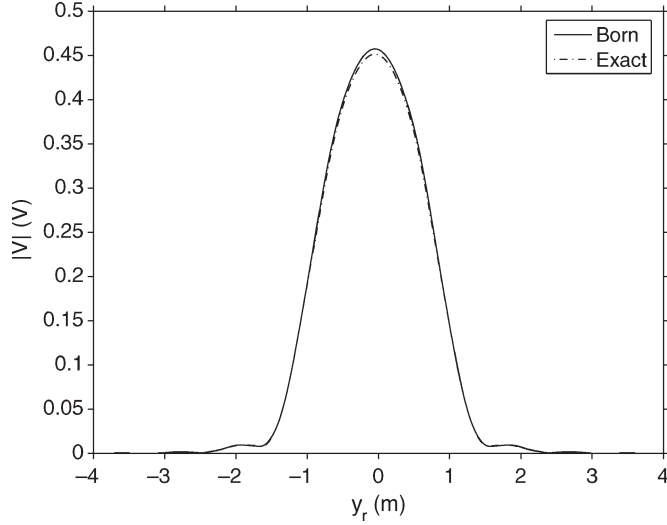
Fig. 2. Magnitude of the output voltage calculated by the Born approximation-based method in this letter and the exact method in [12].
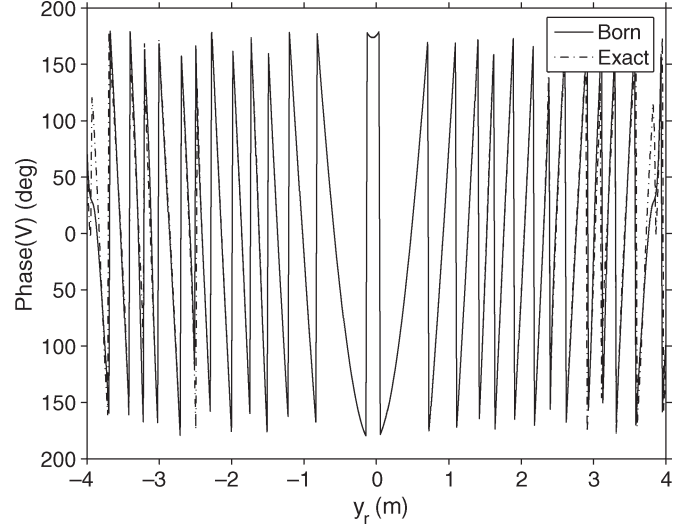

Fig. 3. Phase of the output voltage calculated by the Born approximation-based method in this letter and the exact method in [12].

Assume now that the object is a homogeneous cylinder with permittivity ϵ_s, conductivity σ_s, axis at the depth $z = z_0$, and with rectangular cross section of dimension $2a \times 2b$. In this case, $H(k_y'', z')$ in (24) becomes

$$H\left(k_y'', z'\right) = \int_{-b}^{b} O(z') \exp\left(-ik_y''y'\right) dy'$$
$$= O(z')2b \operatorname{sinc}\left(k_y''b\right) \quad (28)$$

where

$$O(z') = \begin{cases} \sigma_s - \sigma_1 - i\omega(\epsilon_s - \epsilon_1), & |z' - z_0| < a \\ 0, & \text{otherwise.} \end{cases} \quad (29)$$

Similarly, in case the homogeneous cylinder has circular cross section with radius a, $H(k_y'', z')$ becomes

$$H\left(k_y'', z'\right) = 2O(z')\sqrt{a^2 - (z' - z_0)^2}$$
$$\cdot \operatorname{sinc}\left(k_y''\sqrt{a^2 - (z' - z_0)^2}\right). \quad (30)$$

The asymptotic calculation time of the 2.5-D efficient formulation in (22) is $13T_0 N_z N_y^2 \log_2 N_y$ as $N_y \to \infty$, whereas that of the 2.5-D version of the straightforward procedure in (13) is $3N_z N_y^3 \log_2 N_y$. Hence, in the 2.5-D case, the efficient formulation is $3N_y/13$ times faster than the straightforward approach.

V. NUMERICAL INVESTIGATION

To show the correctness of the efficient formulation derived in Section IV, a 2.5-D case involving scattering by a circular cylinder is considered. The radius of the cylinder is 10 cm, its permittivity and conductivity are $\epsilon_s = 8.03\epsilon_0$ and $\sigma_s = 0.01$ S/m, respectively, and it is buried

at $z_0 = -1$ m in soil with $\epsilon_1 = 8\epsilon_0$ and $\sigma_1 = 0.01$ S/m. The antennas of the GPR are $\hat{x}$-directed Hertzian dipoles with an offset of $y_\Delta = 10$ cm and height 5 cm above the soil, and the radar uses the frequency 241 MHz. Equations (22), (23), (25)–(27), and (30) with $V_t = V_{tr} = 1$ V and $Y_0 = 20$ mS are used to calculate the output voltage V of the receiving Hertzian dipole for 660 values of y_r equally spaced between -6 and 6 m.

Figs. 2 and 3 show the magnitude and phase, respectively, of the calculated output voltage compared with the result obtained by using the method described in [12]. The method of [12] is based on an exact eigenfunction expansion of the field scattered by the cylinder. The close agreement between the two results underlines the correctness of the proposed efficient procedure for fixed-offset configurations. The minor discrepancy observed for the magnitude around $y_r = 0$ is due to the limited accuracy of the first-order Born approximation. For the considered configuration, in which $N_y = 660$ observation points are considered, the efficient method derived in this letter is approximately $3N_y/13 \approx 152$ times faster than the straightforward approach.

VI. SUMMARY

An efficient FFT-based formulation is derived for the calculation of linear scattering by buried objects, as involved in the simulation of fixed-offset GPR surveys. The formulation is particularly useful for validation of linear inverse scattering schemes for fixed-offset GPR configurations. For the 3-D case, in which the fixed-offset GPR is placed on a rectangular grid containing $N_x \times N_y$ points, the efficient formulation is approximately $0.75N_x N_y$ times faster than a straightforward evaluation. Similarly, for the 2.5-D case involving N_y observation points, the efficient formulation is $3N_y/13$ times faster. Ongoing research involves the derivation of a similar efficient formulation based on the nonlinear extended Born approximation [13].

REFERENCES

[1] J. E. Molyneux and A. Witten, "Diffraction tomographic imaging in a monostatic measurement geometry," *IEEE Trans. Geosci. Remote Sens.*, vol. 31, no. 2, pp. 507–511, Mar. 1993.

[2] A. Witten, J. E. Molyneux, and J. E. Nyquist, "Ground penetrating radar tomography: Algorithms and case studies," *IEEE Trans. Geosci. Remote Sens.*, vol. 32, no. 2, pp. 461–467, Mar. 1994.

[3] R. Deming and A. J. Devaney, "A filtered backpropagation algorithm for GPR," *J. Environ. Eng. Geophys.*, vol. 1, no. 2, pp. 113–123, Jan. 1996.

[4] ——, "Diffraction tomography for multi-monostatic ground penetrating radar imaging," *Inv. Probl.*, vol. 13, no. 1, pp. 29–45, Feb. 1997.

[5] T. B. Hansen and P. M. Johansen, "Inversion scheme for ground penetrating radar that takes into account the planar air–soil interface," *IEEE Trans. Geosci. Remote Sens.*, vol. 38, no. 1, pp. 496–506, Jan. 2000.

[6] P. Meincke, "Linear GPR inversion for lossy soil and a planar air–soil interface," *IEEE Trans. Geosci. Remote Sens.*, vol. 39, no. 12, pp. 2713–2721, Dec. 2001.

[7] S. K. Lehman, "Superresolution planar diffraction tomography through evanescent fields," *Int. J. Imaging Syst. Technol.*, vol. 12, no. 1, pp. 16–26, Jan. 2002.

[8] J. van der Kruk, C. P. A. Wapenaar, J. T. Fokkema, and P. M. van den Berg, "Three-dimensional imaging of multicomponent ground-penetrating radar data," *Geophysics*, vol. 68, no. 4, pp. 1241–1254, Jul./Aug. 2003.

[9] P. Meincke and T. B. Hansen, "Plane-wave characterization of antennas close to a planar interface," *IEEE Trans. Geosci. Remote Sens.*, vol. 42, no. 6, pp. 1222–1232, Jun. 2004.

[10] H.-R. Lenler-Eriksen and P. Meincke, "Measurement of plane-wave spectra of ground penetrating radar antennas," *Microw. Opt. Technol. Lett.*, vol. 44, no. 3, pp. 215–216, Feb. 2005.

[11] W. C. Chew, *Waves and Fields in Inhomogeneous Media*. Piscataway, NJ: IEEE Press, 1995.

[12] T. B. Hansen and P. Meincke, "Scattering from a buried circular cylinder illuminated by a 3-D source," *Radio Sci.*, vol. 37, no. 2, pp. 41–423, Mar. 2002.

[13] T. M. Habashy, R. W. Groom, and B. R. Spies, "Beyond the Born and Rytov approximations: A nonlinear approach to electromagnetic scattering," *J. Geophys. Res.*, vol. 98, no. B2, pp. 1759–1775, Feb. 1993.